Comput. Aided Geom. Des. 112 (2024) 102361

Contents lists available at ScienceDirect

Computer Aided Geometric Design

journal homepage: www.elsevier.com/locate/cagd

Euler Bézier spirals and Euler B-spline spirals

Xunnian Yang

School of Mathematical Sciences, Zhejiang University, Hangzhou 310058, China

ARTICLE INFO

Keywords:
Bézier curve
B-spline curve
Euler spiral
G^1 interpolation

ABSTRACT

Euler spirals have linear varying curvature with respect to arc length and can be applied in fields such as aesthetics pleasing shape design, curve completion or highway design, etc. However, evaluation and interpolation of Euler spirals to prescribed boundary data is not convenient since Euler spirals are represented by Fresnel integrals but with no closed-form expression of the integrals. We investigate a class of Bézier or B-spline curves called Euler Bézier spirals or Euler B-spline spirals which have specially defined control polygons and approximate linearly varying curvature. This type of spirals can be designed conveniently and evaluated exactly. Simple but efficient algorithms are also given to interpolate G^1 boundary data by Euler Bézier spirals or cubic Euler B-spline spirals.

1. Introduction

Euler spirals, also known as Cornu spirals or Clothoids, are a special type of spirals of which the curvatures vary linearly with respect to arc lengths of the curves. Euler spirals have found wide applications in aesthetics pleasing shape design (Baran et al., 2010; Havemann et al., 2013), shape completion (Kimia et al., 2003; Zhou et al., 2012), highway design or route description of robots (Wang et al., 2001; Ynchausti et al., 2022), etc. Though curvatures of Euler spirals are simple linear functions of arc length, the Cartesian coordinates of Euler spirals are usually represented by Fresnel integrals that have no closed-form solution. Practically, the Cartesian coordinates of Euler spirals have to be evaluated numerically or approximately (Montés et al., 2008; Sánchez-Reyes and Chacón, 2003; Chen et al., 2017; Farouki et al., 2021). When one want to interpolate an Euler spiral to prescribed points and tangents at the boundaries, nonlinear equations will be solved to determine the parameters of the Euler spiral (Walton and Meek, 2009; Bertolazzi and Frego, 2015).

Bézier curves and B-spline curves are polynomial curves or piecewise polynomial curves that can be designed using control polygons and evaluated exactly using the well known de Casteljau algorithm or de Boor algorithm (Farin, 2001). Investigation of Bézier or B-spline curves that have monotone curvature profiles is useful for fair shape design. Frey and Field (2000) studied spirals represented by Bézier conic segments while Dietz and Piper (2004) proposed technique of curve interpolation by cubic spirals. Sufficient conditions for the curvature monotonicity of degree n Bézier curves or B-spline curves have been given in (Wang et al., 2004). Recently, Saito and Yoshida (2023) have presented curvature monotonicity evaluation functions on rational Bézier curves. When the control polygon of a planar Bézier curve is obtained by rotating and scaling edges from previous ones with a constant angle and a constant scaling factor, the Bézier curve can have monotone curvature profile when the rotation angle and the scaling factor are properly chosen (Mineur et al., 1998). Farin (2006) proposed Class A Bézier curves by generalizing typical Bézier curves to 3D space. In recent years, typical or Class A Bézier curves have been studied extensively (Cantón et al., 2021; Romani and Viscardi, 2021;

E-mail address: yxn@zju.edu.cn.

https://doi.org/10.1016/j.cagd.2024.102361
Received 25 July 2023; Received in revised form 13 March 2024; Accepted 3 June 2024

Available online 7 June 2024

Tong and Chen, 2021; Wang et al., 2023). It is noticed that planar typical or Class A Bézier curves are approximants to logarithmic spirals and they can converge to logarithmic spirals when the degrees of Bézier curves are increased (Yoshida et al., 2008).

Similar to planar typical or Class A Bézier curves that employ discrete logarithmic spirals as control polygons, we propose to construct planar Bézier curves or planar B-spline curves by employing Euler spiral-like control polygons that have equal-length edges and linearly varying vertex angles. Just like discrete Euler spirals which are approximants to Euler spirals, the defined polygons are also approximants to Euler spirals. Consequently, the Bézier curves or B-spline curves constructed by the polygons are approximants to Euler spirals too. This makes it possible to construct Bézier curves or B-spline curves with monotone curvature profiles by choosing proper parameters for the specially defined control polygons. If the control polygons have increased numbers of vertices but reduced maximum vertex angles, then the polygons can approximate Euler spirals with even higher accuracy while the obtained Bézier or B-spline curves lie much closer to the control polygons. It follows that the constructed Bézier curves or B-spline curves can have approximate linearly varying curvature profiles with respect to the parameter. Since this type of Bézier or B-spline curves behave like Euler spirals, we refer the curves as *Euler Bézier spirals* or *Euler B-spline spirals*. Unlike planar typical Bézier curves that can only be used to model local convex curves, Euler Bézier spirals and Euler B-spline spirals can be employed to model convex curves as well as curves with inflections. Given a pair of G^1 boundary data, an interpolating Euler Bézier spiral or Euler B-spline spiral can be obtained efficiently by smoothing rough control polygons and inserting new control points iteratively.

The paper is organized as follows. In Section 2 we review some basic properties of Euler spirals and discrete Euler spirals. In Section 3 we propose definitions of Euler Bézier spirals and Euler B-spline spirals. Algorithms for G^1 interpolation by Euler Bézier spirals or Euler B-spline spirals will be given in Section 4. In Section 5 we present several interesting examples for curve and surface modeling by the proposed models and Section 6 concludes the paper with a brief summary.

2. Background

Our proposed special types of Bézier curves and B-spline curves are closely related with intrinsic definition of Euler spirals as well as discrete Euler spirals.

The curvature k of an Euler spiral can be represented as a linear function of its arc length s as

$$k(s) = as + b, \tag{1}$$

where $a \in \mathbb{R}$ and $b \in \mathbb{R}$ are constants. If $a = 0$, the spiral reduces to a circle or a line with constant curvature b; otherwise, the spiral has a single inflection point at $s = -\frac{b}{a}$. By integral of curvature, the tangent or winding angle Φ with respect to arc length is obtained as

$$\Phi(s) = \frac{1}{2}as^2 + bs + c, \tag{2}$$

where c is the tangent angle at $s = 0$. Based on the expression of tangent angle, the unit tangent direction of the Euler spiral at s is given by

$$T(s) = \begin{pmatrix} \cos(\Phi(s)) \\ \sin(\Phi(s)) \end{pmatrix}.$$

The integral of $T(s)$ gives the Cartesian coordinates of Euler spiral as

$$Q(s) = \int_0^s T(u)du.$$

However, the integral has no closed-form expression when $a \neq 0$, numerical techniques have to be employed to evaluate the points on the curve.

Assume $s_i = s_0 + i\Delta s$, $i = 0, 1, \ldots, n$, are a sequence of sampled parameters with a fixed arc length step Δs. A polygon $Q(s_0)Q(s_1)\cdots Q(s_n)$ is obtained as a discrete Euler spiral. For each $0 < i < n$, the turning angle θ_i at vertex $Q(s_i)$ is estimated as the angle between tangent vector $T(s_{i-\frac{1}{2}})$ and tangent vector $T(s_{i+\frac{1}{2}})$, where $s_{i+\frac{1}{2}} = \frac{1}{2}(s_i + s_{i+1})$. We have

$$\theta_i := \Phi(s_{i+\frac{1}{2}}) - \Phi(s_{i-\frac{1}{2}}) = a(\Delta s)^2 i + a(\Delta s)s_0 + b\Delta s, \quad i = 1, 2, \ldots, n-1.$$

The angle θ_i is positive when the tangent vector is winding counter-clockwise at $Q(s_i)$ and negative otherwise. If all θ_is have absolutely small values, the polygon $Q(s_0)Q(s_1)\cdots Q(s_n)$ has nearly equal-length edges and linearly varying vertex angles. Assume $a \neq 0$ and denote $a(\Delta s)^2 = \Delta\theta$, it yields that $\theta_i - \theta_{i-1} = \Delta\theta$, $i = 2, 3, \ldots, n-1$. Because $k'(s) = a$ and $\Delta\theta$ have the same sign, the curvature of an Euler spiral increases when $\Delta\theta > 0$ and decreases when $\Delta\theta < 0$.

Motivated by discrete Euler spirals, an Euler spiral-like polygon or *Euler polygon* is defined as follows.

Definition 2.1. Assume $n \geq 3$ is an integer and $P_0P_1 \ldots P_n$ is a planar polygon. Assume θ_is are the signed angles from vector $P_{i-1}P_i$ to vector P_iP_{i+1}, $i = 1, 2, \ldots, n-1$. If the edges and the vertex angles of the polygon satisfy $\|P_i - P_{i-1}\| = \|P_{i+1} - P_i\|$, $\theta_i = \theta_1 + (i-1)\Delta\theta$, $i = 1, 2, \ldots, n-1$, the polygon is referred as an Euler polygon.

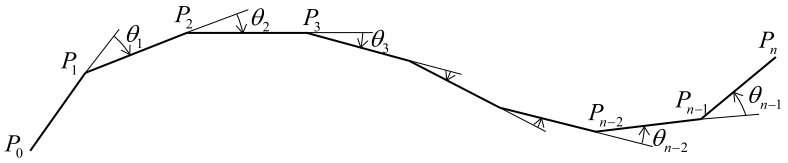

Fig. 1. An Euler polygon with equal-length edges and linearly varying vertex angles.

Let

$$\mathrm{R}(\theta) = \begin{pmatrix} \cos\theta & -\sin\theta \\ \sin\theta & \cos\theta \end{pmatrix}.$$

Then $\mathrm{R}(\theta)\mathbf{v}$ represents a vector obtained by rotating vector $\mathbf{v}$ with angle θ. Particularly, if $\theta > 0$ the rotation is counter-clockwise; otherwise, the rotation is clockwise. Given integer $n \geq 3$, vector $\mathbf{v}$, real numbers θ_1 and $\Delta\theta$, the vertices of an Euler polygon starting from point P_0 can be obtained by

$$\begin{cases} P_1 &= P_0 + \mathbf{v}, \\ P_i &= P_{i-1} + \mathrm{R}(\theta_1 + \cdots + \theta_{i-1})\mathbf{v}, \quad i = 2, 3, \ldots, n, \end{cases} \tag{3}$$

where $\theta_i = \theta_1 + (i-1)\Delta\theta$, $i = 2, \ldots, n-1$. Notice that $\mathrm{R}(\theta_1 + \cdots + \theta_{i-1}) = \mathrm{R}(\theta_{i-1}) \cdots \mathrm{R}(\theta_1)$, the second equality in Equation (3) can also be reformulated as $P_i - P_{i-1} = \mathrm{R}(\theta_{i-1})(P_{i-1} - P_{i-2})$, $i = 2, 3, \ldots, n$. This means that the edges of an Euler polygon can be obtained by rotating previous edges sequentially. See Fig. 1 for an example of Euler polygon. From the definition of Euler polygons we know that an Euler polygon is approximately a discrete Euler spiral and it can approximate an Euler spiral even closely when the polygon is defined by increased number of vertices and absolutely smaller vertex angles. In next section we will show that Bézier or B-spline curves constructed with Euler polygons can be spirals when the vertex angles have been properly chosen.

3. Euler Bézier/B-spline spirals

In this section we construct Bézier or B-spline curves by choosing Euler polygons as control polygons. Simple necessary conditions for judging the curvature monotonicity of such Bézier or B-spline curves are given.

3.1. Euler Bézier spirals

Assume P_0, P_1, …, P_n are a sequence of points given by Equation (3), a Bézier curve is obtained as $P(t) = \sum_{i=0}^{n} P_i B_{i,n}(t)$, where $B_{i,n}(t) = \frac{n!}{i!(n-i)!} t^i (1-t)^{n-i}$, $i = 0, 1, \ldots, n$, are Bernstein basis functions. To judge whether or not the Bézier curve is a spiral, the curvature and the curvature derivative will be computed.

Under the assumption that the control polygon is an Euler polygon, the first order derivative of a Bézier curve of degree n is computed as

$$P'(t) = n \sum_{i=0}^{n-1} \Delta P_i B_{i,n-1}(t),$$

where $\Delta P_0 = P_1 - P_0 = \mathbf{v}$, $\Delta P_i = P_{i+1} - P_i = \mathrm{R}(\theta_1 + \cdots + \theta_i)\mathbf{v}$, $i = 1, \ldots, n-1$. Consequently, the second order derivative of the Bézier curve is

$$P''(t) = n(n-1) \sum_{i=0}^{n-2} \Delta^2 P_i B_{i,n-2}(t),$$

where $\Delta^2 P_0 = \Delta P_1 - \Delta P_0 = \mathrm{R}(\theta_1)\mathbf{v} - \mathbf{v}$, $\Delta^2 P_i = \Delta P_{i+1} - \Delta P_i = \mathrm{R}(\theta_1 + \cdots + \theta_{i+1})\mathbf{v} - \mathrm{R}(\theta_1 + \cdots + \theta_i)\mathbf{v}$, $i = 1, 2, \ldots, n-2$.

To compute curvature and curvature derivative of the curve $P(t)$, we will have to compute $U(t) = P'(t) \wedge P''(t)$ and $V(t) = \|P'(t)\|^2$, where "$\wedge$" represents the scalar cross product of two planar vectors and $\|\cdot\|$ represents the Euclidean norm of a vector. Assume $\|\mathbf{v}\| = l$. From the derivatives of the Bézier curve, it yields that

$$\begin{aligned} U(t) = n^2(n-1)l^2 \Bigg\{ & \sin\theta_1 B_{0,2n-3}(t) + \left[\frac{n-2}{2n-3} \sin(\theta_1 + \theta_2) + \frac{1}{2n-3} \sin\theta_1 \right] B_{1,2n-3}(t) + \cdots \\ & + \left[\frac{n-2}{2n-3} \sin(\theta_{n-2} + \theta_{n-1}) + \frac{1}{2n-3} \sin\theta_{n-1} \right] B_{2n-4,2n-3}(t) + \sin\theta_{n-1} B_{2n-3,2n-3}(t) \Bigg\} \end{aligned}$$

and

$$V(t) = n^2 l^2 \left[B_{0,2n-2}(t) + \cos\theta_1 B_{1,2n-2}(t) + \cdots + \cos\theta_{n-1} B_{2n-3,2n-2}(t) + B_{2n-2,2n-2}(t) \right].$$

Now, the curvature of the curve is computed by

$$k(t) = \frac{P'(t) \wedge P''(t)}{(\|P'(t)\|^2)^{\frac{3}{2}}} = \frac{U(t)}{V(t)^{\frac{3}{2}}} \tag{4}$$

and the derivative of curvature is obtained as

$$k'(t) = \frac{U'(t)V(t) - \frac{3}{2}U(t)V'(t)}{V(t)^{\frac{5}{2}}}. \tag{5}$$

Particularly, by choosing $t = 0$ or $t = 1$, the curvatures and the curvature derivatives at the boundaries of the Bézier curve are obtained as

$$k(0) = \frac{n-1}{n}\frac{\sin\theta_1}{l}, \quad k(1) = \frac{n-1}{n}\frac{\sin\theta_{n-1}}{l}$$

and

$$k'(0) = \frac{n-1}{nl}[(n+1)\sin\theta_1 + (n-2)\sin(\theta_1+\theta_2) - 3(n-1)\sin\theta_1\cos\theta_1],$$
$$k'(1) = \frac{n-1}{nl}[-(n+1)\sin\theta_{n-1} - (n-2)\sin(\theta_{n-2}+\theta_{n-1}) + 3(n-1)\sin\theta_{n-1}\cos\theta_{n-1}].$$

It is known that the curvature derivative $k'(t) \geq 0$ or $k'(t) \leq 0$, $t \in [0,1]$, and the curvature difference $k(1) - k(0) > 0$ or $k(1) - k(0) < 0$ when the curvature plot is monotone increasing or monotone decreasing, respectively. Consequently, if $k'(0)$ or $k'(1)$ has an opposite sign with $k(1) - k(0)$, the Bézier curve is not a spiral. To construct a Bézier curve with monotone curvature, we assume all vertex angles of the control polygon are acute angles. Under this assumption, we know that the sign of $k(1) - k(0) = \frac{n-1}{nl}(\sin\theta_{n-1} - \sin\theta_1)$ is equal to the sign of $\theta_{n-1} - \theta_1$, or equivalently, the sign of $\Delta\theta$. As our main goal is to construct Bézier or B-spline curves that have approximately linear curvature by using Euler polygons, we assume further that the curvature derivative of a Bézier spiral satisfies $k'(t) \neq 0$, $t \in [0,1]$, which implies that $k'(t)$ and $k(1) - k(0)$ have the same sign. However, the sign of function $k'(t)$, $0 \leq t \leq 1$, is not easily judged. It is based on the sign of a curvature monotone variation function of degree $4n-6$ for degree n Bézier curves generally (Wang et al., 2004). Based on the expressions of $k'(0)$ and $k'(1)$, we present here a simple necessary condition for checking the curvature monotonicity of the Bézier curve with Euler control polygon.

Proposition 3.1. *Assume $P(t) = \sum_{i=0}^{n} P_i B_{i,n}(t)$, $0 \leq t \leq 1$, is a Bézier curve of degree n and the control points form an Euler polygon. Assume $\theta_i = \theta_1 + (i-1)\Delta\theta$, $i = 1, 2, \ldots, n-1$, are the vertex angles of the polygon and satisfy $|\theta_i| < \frac{\pi}{2}$, $i = 1, 2, \ldots, n-1$. Let $s_0 = (n+1)\sin\theta_1 + (n-2)\sin(\theta_1+\theta_2) - 3(n-1)\sin\theta_1\cos\theta_1$ and $s_1 = -(n+1)\sin\theta_{n-1} - (n-2)\sin(\theta_{n-2}+\theta_{n-1}) + 3(n-1)\sin\theta_{n-1}\cos\theta_{n-1}$. If the Bézier curve $P(t)$ is a spiral with curvature derivative $k'(t) \neq 0$, $t \in [0,1]$, then $\Delta\theta$, s_0 and s_1 have the same sign.*

Remark. Based on Proposition 3.1 we know that a Bézier curve with Euler control polygon is not a spiral when $\Delta\theta$, s_0 and s_1 have different signs. If $\Delta\theta$, s_0 and s_1 have the same sign, the obtained Bézier curves are always spirals, as long as we have experimented. Actually, by dense sampling of curvatures or curvature derivatives on the domain, it is verified that $k'(t) > 0$ or $k'(t) < 0$, $0 \leq t \leq 1$, always holds when $\Delta\theta$, s_0 and s_1 have the same positive sign or the same negative sign, respectively. However, a rigorous proof of this assertion is missing at present. We call the Bézier curves satisfying Proposition 3.1 *Euler Bézier spirals*.

Proposition 3.2. *Assume $n_0 \geq 3$ is an integer and $\Gamma_n = P_0^n P_1^n \ldots P_n^n$, $n = n_0, n_0+1, \ldots$, are a sequence of Euler polygons. If the polygons Γ_n, $n = n_0, n_0+1, \ldots$, converge to a segment of Euler spiral when n approaches infinity, then the Bézier curves $P_n(t) = \sum_{i=0}^{n} P_i^n B_{i,n}(t)$, $t \in [0,1]$, $n = n_0, n_0+1, \ldots$, converge to the same Euler spiral segment.*

Proof. Assume each Euler polygon Γ_n is represented as a piecewise linear function $\Gamma_n(t)$ with vertices $P_i^n = \Gamma_n(\frac{i}{n})$, $i = 0, 1, \ldots, n$, and $\lim_{n\to\infty}\Gamma_n(t) = \mathbf{r}(t)$, $t \in [0,1]$, where $\mathbf{r}(t)$ is a segment of Euler spiral, then the vertices of Γ_n can be represented as $P_i^n = \mathbf{r}(\frac{i}{n}) + \varepsilon_i^n$, where the residuals ε_i^ns satisfy $\lim_{n\to\infty}\max_{0\leq i\leq n}\|\varepsilon_i^n\| = 0$. Consequently, the Bézier curve $P_n(t)$ can be reformulated as

$$P_n(t) = \sum_{i=0}^{n}\left[\mathbf{r}\left(\frac{i}{n}\right) + \varepsilon_i^n\right]B_{i,n}(t) = \sum_{i=0}^{n}\mathbf{r}\left(\frac{i}{n}\right)B_{i,n}(t) + \sum_{i=0}^{n}\varepsilon_i^n B_{i,n}(t).$$

Based on Bernstein's approximation theorem, we know that $\lim_{n\to\infty}\sum_{i=0}^{n}\mathbf{r}(\frac{i}{n})B_{i,n}(t) = \mathbf{r}(t)$, $t \in [0,1]$. Under the condition that $\lim_{n\to\infty}\max_{0\leq i\leq n}\|\varepsilon_i^n\| = 0$, we have $\lim_{n\to 0}\sum_{i=0}^{n}\varepsilon_i^n B_{i,n}(t) = 0$, $t \in [0,1]$. Combining these two limits together, we have $\lim_{n\to\infty}P_n(t) = \mathbf{r}(t)$, $t \in [0,1]$. This proves the proposition. □

From Proposition 3.2 we know that a Bézier curve with Euler control polygon can approximate an Euler spiral well when the control polygon approximates the Euler spiral with a high accuracy. In case a Bézier curve with Euler control polygon is not a spiral, one can increase the number of control points and recompute the Euler control polygon with fixed boundary points and boundary tangents. This process can be iterated, until an Euler Bézier spiral has been obtained. In next section, an algorithm for constructing

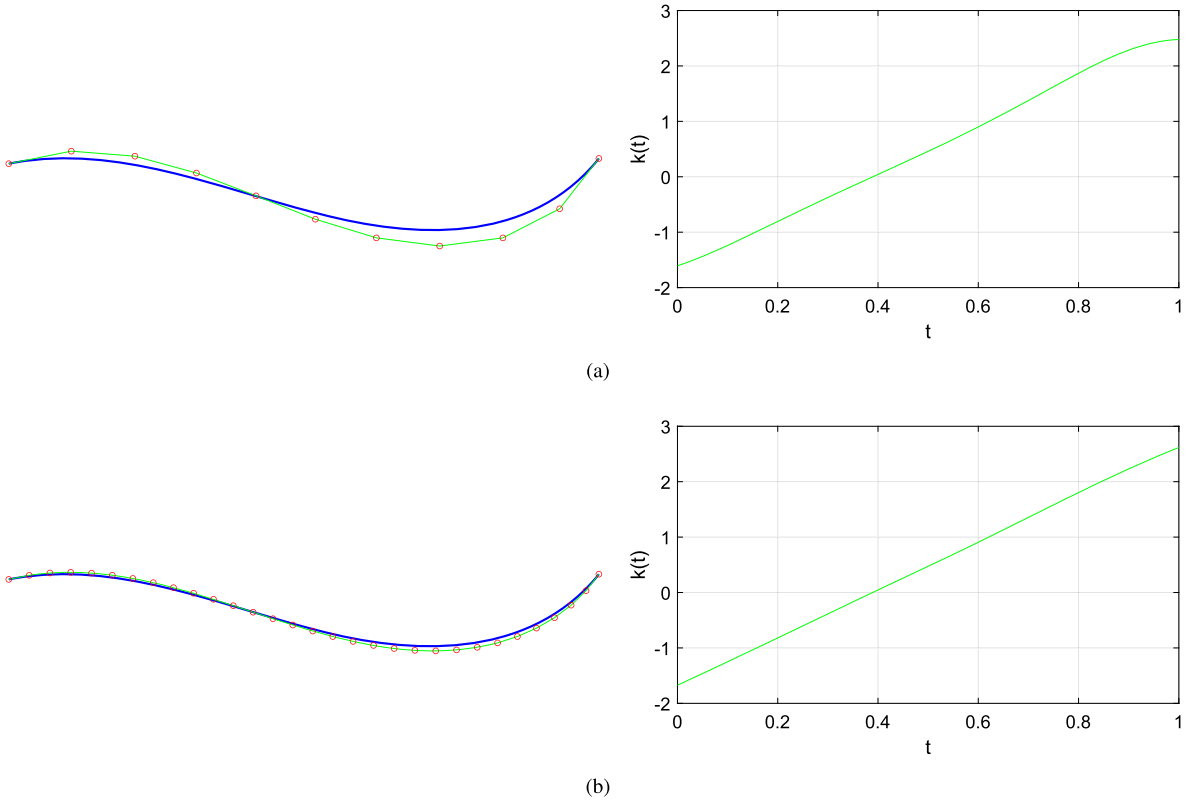

Fig. 2. (a) An Euler Bézier spiral of degree 10 and its curvature plot; (b) an Euler Bézier spiral of degree 30 and its curvature plot.

G^1 interpolating Euler Bézier spirals by elevating degrees and recomputing Euler control polygons from rough initial Bézier curves will be given.

Fig. 2(a) illustrates an Euler Bézier curve of degree 10. With control polygon satisfying necessary conditions stated in Proposition 3.1, the obtained Bézier curve is a spiral. The curvature plot of the curve demonstrates this observation. If we construct an Euler Bézier curve with even a higher degree and fixed boundary points and boundary tangents, the curve can lie closer to the control polygon and the curvature plot can be approximately linear. See Fig. 2(b) for an Euler Bézier spiral of degree 30 and its curvature plot.

3.2. Euler B-spline spirals

Just like Euler Bézier spirals, B-spline curves constructed with Euler polygons can also be spirals. Assume P_0, P_1, …, P_n are the vertices of an Euler polygon and $\theta_i = \theta_1 + (i-1)\Delta\theta$, $i = 1, 2, \dots, n-1$, are the signed vertex angles of the polygon. A uniform B-spline curve of order k (degree $k-1$) is obtained as $P(t) = \sum_{i=0}^{n} P_i N_{i,k}(t)$, where $N_{i,k}(t)$, $i = 0, 1, \dots, n$, are the B-spline basis functions defined on knot vector $\tau = \{t_0, t_0+1, \dots, t_0+n+k\}$, with $t_0 \in \mathbb{R}$. Though all B-spline curves of degree greater than or equal to 3 can be spirals, we derive here conditions under which cubic B-spline curves are spirals. This is because cubic B-spline curves are popular in practice. As seen later, control points of cubic Euler B-spline spirals can be derived in an efficient way to interpolate prescribed G^1 boundary data.

Since B-spline curves are piecewise polynomials, we first derive conditions for curvature monotonicity of one piece of cubic B-spline curve. After then, the conditions for checking curvature monotonicity of a whole cubic B-spline curve will be given. W.l.o.g, we assume a piece of cubic B-spline curve is given by $P(t) = \sum_{j=0}^{3} P_j N_{j,4}(t)$, $t \in [0,1]$, where $N_{0,4}(t) = \frac{1}{6}(1-t)^3$, $N_{1,4}(t) = \frac{1}{6}(3t^3 - 6t^2 + 4)$, $N_{2,4}(t) = \frac{1}{6}(-3t^3 + 3t^2 + 3t + 1)$ and $N_{3,4}(t) = \frac{1}{6}t^3$. For ease of computation of curvatures and curvature derivatives at the boundaries we reformulate the B-spline curve as a cubic Bézier curve $P(t) = \sum_{j=0}^{3} Q_j B_{j,3}(t)$, where $Q_0 = P_1 + \frac{1}{6}(P_0 - P_1 + P_2 - P_1)$, $Q_1 = \frac{2}{3}P_1 + \frac{1}{3}P_2$, $Q_2 = \frac{1}{3}P_1 + \frac{2}{3}P_2$ and $Q_3 = P_2 + \frac{1}{6}(P_1 - P_2 + P_3 - P_2)$. Fig. 3 illustrates a piece of cubic B-spline curve with Euler control polygon and the converted Bézier curve.

Denote $P_1 - P_0 = \mathbf{v}$, $P_2 - P_1 = \mathrm{R}(\theta_1)\mathbf{v}$ and $P_3 - P_2 = \mathrm{R}(\theta_1 + \theta_2)\mathbf{v}$. The first order derivative of the Bézier curve is obtained as

$$P'(t) = 3\sum_{j=0}^{2} \Delta Q_j B_{j,2}(t),$$

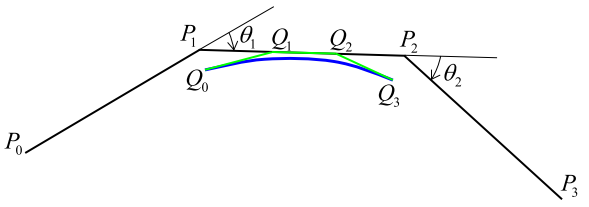

Fig. 3. Conversion of a piece of cubic B-spline curve to a Bézier curve.

where $\Delta Q_0 = Q_1 - Q_0 = \frac{1}{6}\mathbf{v} + \frac{1}{6}\mathrm{R}(\theta_1)\mathbf{v}$, $\Delta Q_1 = Q_2 - Q_1 = \frac{1}{3}\mathrm{R}(\theta_1)\mathbf{v}$ and $\Delta Q_2 = Q_3 - Q_2 = \frac{1}{6}\mathrm{R}(\theta_1)\mathbf{v} + \frac{1}{6}\mathrm{R}(\theta_1+\theta_2)\mathbf{v}$. Further more, the second order derivative of the curve is computed by

$$P''(t) = 6\Delta^2 Q_0 B_{0,1}(t) + 6\Delta^2 Q_1 B_{1,1}(t),$$

where $\Delta^2 Q_0 = \frac{1}{6}[\mathrm{R}(\theta_1)\mathbf{v} - \mathbf{v}]$ and $\Delta^2 Q_1 = \frac{1}{6}[\mathrm{R}(\theta_1+\theta_2)\mathbf{v} - \mathrm{R}(\theta_1)\mathbf{v}]$. Based on the computed derivatives, and let $l = \|\mathbf{v}\|$, we have

$$\begin{aligned} U(t) &= P'(t) \wedge P''(t) \\ &= l^2 \left\{ \sin\theta_1 B_{0,3}(t) + \left[\frac{1}{2}\sin\theta_1 + \frac{1}{6}\sin(\theta_1+\theta_2) + \frac{1}{6}\sin\theta_2\right] B_{1,3}(t) \right. \\ &\quad \left. + \left[\frac{1}{6}\sin\theta_1 + \frac{1}{6}\sin(\theta_1+\theta_2) + \frac{1}{2}\sin\theta_2\right] B_{2,3}(t) + \sin\theta_2 B_{3,3}(t) \right\} \end{aligned}$$

and

$$\begin{aligned} V(t) &= \left[P'(t)\right]^2 \\ &= l^2 \left[\frac{1}{2}(1+\cos\theta_1)B_{0,4}(t) + \frac{1}{2}(1+\cos\theta_1)B_{1,4}(t) + \cdots + \frac{1}{2}(1+\cos\theta_2)B_{3,4}(t) + \frac{1}{2}(1+\cos\theta_2)B_{4,4}(t)\right]. \end{aligned}$$

Substituting above $U(t)$ and $V(t)$ into Equation (4) and Equation (5), the curvatures and the curvature derivatives at the ends of the cubic B-spline segment are obtained as

$$k(0) = \frac{2\sin\frac{\theta_1}{2}}{l\cos^2\frac{\theta_1}{2}}, \qquad k(1) = \frac{2\sin\frac{\theta_2}{2}}{l\cos^2\frac{\theta_2}{2}} \tag{6}$$

and

$$k'(0) = \frac{1}{l\cos^2\frac{\theta_1}{2}}\left[-3\sin\frac{\theta_1}{2} + \sin\left(\frac{\theta_1}{2}+\theta_2\right)\right], \qquad k'(1) = \frac{1}{l\cos^2\frac{\theta_2}{2}}\left[3\sin\frac{\theta_2}{2} - \sin\left(\theta_1+\frac{\theta_2}{2}\right)\right]. \tag{7}$$

Assume the two vertex angles of the control polygon of a piece of cubic B-spline curve satisfy $|\theta_1| < \frac{\pi}{2}$ and $|\theta_2| < \frac{\pi}{2}$. Let $f(\theta) = \frac{2\sin\theta}{l\cos^2\theta}$. It yields that $f'(\theta) = \frac{2}{l}\frac{1+\sin^2\theta}{\cos^3\theta} > 0$ for $\theta \in (-\frac{\pi}{2}, \frac{\pi}{2})$. Since $f(\theta)$ is monotone increasing, from Equation (6), we know that $k(1) - k(0) = f(\frac{\theta_2}{2}) - f(\frac{\theta_1}{2})$ and $\theta_2 - \theta_1$ have the same sign. Then, a necessary condition for judging the curvature monotonicity of one piece of cubic B-spline curve is obtained as follows.

Proposition 3.3. *Assume $P(t) = \sum_{j=0}^{3} P_j N_{j,4}(t)$, $0 \le t \le 1$, is a piece of cubic B-spline curve and the control points form an Euler polygon. Assume the two vertex angles satisfy $|\theta_1| < \frac{\pi}{2}$, $|\theta_2| < \frac{\pi}{2}$ and $\theta_1 \neq \theta_2$. Let $h_0 = -3\sin\frac{\theta_1}{2} + \sin(\frac{\theta_1}{2}+\theta_2)$ and $h_1 = 3\sin\frac{\theta_2}{2} - \sin(\theta_1 + \frac{\theta_2}{2})$. If the cubic B-spline segment $P(t)$ is a spiral with curvature derivative $k'(t) \neq 0$, $0 \le t \le 1$, then $\theta_2 - \theta_1$, h_0 and h_1 have the same sign.*

Practically, a cubic B-spline segment $P(t)$ as defined in Proposition 3.3 is always a spiral when the signs of $\theta_2 - \theta_1$, h_0 and h_1 are the same. Then the necessary condition in Proposition 3.3 can be employed to judge whether or not a piece of cubic B-spline curve with Euler control polygon is a spiral. In case the control polygon of the cubic B-spline segment is inflectional, the signs of curvature derivatives at the ends of the curve segment can be obtained directly from the relationship between two vertex angles.

Proposition 3.4. *Assume $P(t)$ is a piece of cubic B-spline curve stated in Proposition 3.3. If the two vertex angles of the control polygon satisfy $-\frac{\pi}{2} < \theta_1 < 0 < \theta_2 < \frac{\pi}{2}$, then $k'(0) > 0$ and $k'(1) > 0$. Similarly, if $-\frac{\pi}{2} < \theta_2 < 0 < \theta_1 < \frac{\pi}{2}$, then $k'(0) < 0$ and $k'(1) < 0$.*

Proof. We prove the inequalities $k'(0) > 0$ and $k'(1) > 0$. The inequalities $k'(0) < 0$ and $k'(1) < 0$ can be proved similarly.

Under the assumption that $-\frac{\pi}{2} < \theta_1 < 0 < \theta_2 < \frac{\pi}{2}$, we have $-\frac{\pi}{4} < \frac{\theta_1}{2} < \frac{\theta_1}{2} + \theta_2 < \theta_2 < \frac{\pi}{2}$ and $-\frac{\pi}{2} < \theta_1 < \theta_1 + \frac{\theta_2}{2} < \frac{\theta_2}{2} < \frac{\pi}{4}$. It yields that

$$\sin\left(\frac{\theta_1}{2}+\theta_2\right) > \sin\left(\frac{\theta_1}{2}\right) > 3\sin\left(\frac{\theta_1}{2}\right)$$

and

$$3\sin\left(\frac{\theta_2}{2}\right) > \sin\left(\frac{\theta_2}{2}\right) > \sin\left(\theta_1+\frac{\theta_2}{2}\right).$$

From Equation (7) we have $k'(0)>0$ and $k'(1)>0$. This completes the proof. □

Based on Proposition 3.4 we know that a piece of cubic B-spline curve with inflectional Euler control polygon is a spiral when the two angles at the intermediate vertices are acute angles.

For a cubic B-spline curve with more than 4 control points, the curve is consisting of two or more pieces of cubic curves. If every piece of the cubic B-spline curve is a spiral and curvature derivatives of all spirals have the same sign, the B-spline curve is referred as a cubic B-spline spiral. Particularly, if the control polygon of a cubic B-spline curve is an Euler polygon, whether or not the B-spline curve is a spiral should just be judged by checking the curvature monotonicity of the first and the last segments of the cubic B-spline curve.

Proposition 3.5. *Assume $n>=4$ is an integer and planar polygon $P_0P_1\dots P_n$ is an Euler polygon with vertex angles satisfying $\theta_k=\theta_1+(k-1)\Delta\theta$, $|\theta_k|<\frac{\pi}{2}$, $k=1,2,\dots,n-1$. Assume $C_i(u)=P_{i-1}N_{0,4}(u)+P_iN_{1,4}(u)+P_{i+1}N_{2,4}(u)+P_{i+2}N_{3,4}(u)$, $0\le u\le 1$, $i=1,2,\dots,n-2$, are pieces of cubic B-spline curves defined by the Euler polygon. Denote the curvatures of the B-spline segments as $k_i(u)$, $i=1,2,\dots,n-2$. Let $F_0(\theta)=-3\sin\frac{\theta}{2}+\sin(\frac{3\theta}{2}+\Delta\theta)$ and $F_1(\theta)=3\sin\frac{\theta}{2}-\sin(\frac{3\theta}{2}-\Delta\theta)$. The signs of curvature derivatives can be judged as follows.*

(1) *If $\Delta\theta>0$, $F_0(\theta_1)>0$, $F_1(\theta_2)>0$, $F_0(\theta_{n-2})>0$ and $F_1(\theta_{n-1})>0$, then $k_i'(0)>0$, $k_i'(1)>0$, $i=1,2,\dots,n-2$.*
(2) *If $\Delta\theta<0$, $F_0(\theta_1)<0$, $F_1(\theta_2)<0$, $F_0(\theta_{n-2})<0$ and $F_1(\theta_{n-1})<0$, then $k_i'(0)<0$, $k_i'(1)<0$, $i=1,2,\dots,n-2$.*

Proof. We prove the B-spline spirals with monotone increasing curvature profiles, the B-spline spirals with monotone decreasing curvature profiles can be proved in the same way.

Based on Equation (7), we know that the curvature derivatives at the ends of the cubic B-spline segments are

$$k_i'(0)=\frac{1}{l\cos^2\frac{\theta_i}{2}}F_0(\theta_i),\quad k_i'(1)=\frac{1}{l\cos^2\frac{\theta_{i+1}}{2}}F_1(\theta_{i+1}),\qquad i=1,2,\dots,n-2. \tag{8}$$

From their definition, the derivatives of $F_0(\theta)$ and $F_1(\theta)$ are obtained as

$$F_0'(\theta)=-\frac{3}{2}\cos\frac{\theta}{2}+\frac{3}{2}\cos\left(\frac{3\theta}{2}+\Delta\theta\right)=-3\sin\left(\theta+\frac{\Delta\theta}{2}\right)\sin\left(\frac{\theta}{2}+\frac{\Delta\theta}{2}\right),$$
$$F_1'(\theta)=\frac{3}{2}\cos\frac{\theta}{2}-\frac{3}{2}\cos\left(\frac{3\theta}{2}-\Delta\theta\right)=3\sin\left(\theta-\frac{\Delta\theta}{2}\right)\sin\left(\frac{\theta}{2}-\frac{\Delta\theta}{2}\right).$$

If $F_0(\theta_1)>0$, $F_1(\theta_2)>0$, $F_0(\theta_{n-2})>0$ and $F_1(\theta_{n-1})>0$, it yields that $k_1'(0)>0$, $k_1'(1)>0$, $k_{n-2}'(0)>0$ and $k_{n-2}'(1)>0$. To prove that $k_i'(0)>0$, $k_i'(1)>0$, $i=2,3,\dots,n-3$, we should prove that $F_0(\theta_i)>0$ and $F_1(\theta_{i+1})>0$, $i=2,3,\dots,n-3$. We show that the inequalities hold in following two subcases.

(a) The vertex angles satisfy $0<\theta_1<\theta_2<\cdots<\theta_{n-1}<\frac{\pi}{2}$ or $-\frac{\pi}{2}<\theta_1<\theta_2<\cdots<\theta_{n-1}<0$.

In this case all vertex angles have the same sign. From the expressions of $F_0'(\theta)$ and $F_1'(\theta)$, we know that $F_0'(\theta)<0$ when $\theta\in[\theta_1,\theta_{n-2}]$ and $F_1'(\theta)>0$ when $\theta\in[\theta_2,\theta_{n-1}]$. Since $F_0(\theta_{n-2})>0$ and $F_0(\theta)$ is monotone decreasing, we have $F_0(\theta_1)>F_0(\theta_2)>\cdots>F_0(\theta_{n-2})>0$. Because $F_1(\theta_2)>0$ and $F_1(\theta)$ is monotone increasing, we have $0<F_1(\theta_2)<F_1(\theta_3)<\cdots<F_1(\theta_{n-1})$. From Equation (8) we know that $k_i'(0)>0$, $k_i'(1)>0$ when $i=2,3,\dots,n-3$.

(b) The vertex angles satisfy $-\frac{\pi}{2}<\theta_1<\cdots<\theta_{i_0}<0<\theta_{i_0+1}<\cdots<\theta_{n-1}<\frac{\pi}{2}$.

Based on Proposition 3.4 we know that $k_{i_0}'(0)>0$ and $k_{i_0}'(1)>0$. It follows that $F_0(\theta_{i_0})>0$ and $F_1(\theta_{i_0+1})>0$. To prove the proposition, we should prove that $F_0(\theta_i)>0$, $i=1,2,\dots,i_0-1,i_0+1,\dots,n-2$, and $F_1(\theta_i)>0$, $i=2,3,\dots,i_0,i_0+2,\dots,n-1$. By direct computation, we know that $F_0'(-\Delta\theta)=0$ and $F_0''(-\Delta\theta)=\frac{3}{2}\sin\frac{\Delta\theta}{2}>0$. It follows that $F_0'(\theta)<0$ when $\theta\in[\theta_1,-\Delta\theta)$. Since $\theta_{i_0-1}=\theta_{i_0}-\Delta\theta<-\Delta\theta$, we have

$$F_0(\theta_1)>F_0(\theta_2)>\cdots>F_0(\theta_{i_0-1})>F_0(-\Delta\theta)=2\sin\frac{\Delta\theta}{2}>0.$$

On the other hand, since $F_0'(\theta)<0$ when $\theta\in[\theta_{i_0+1},\theta_{n-2}]$, we have

$$F_0(\theta_{i_0+1})>F_0(\theta_{i_0+2})>\cdots>F_0(\theta_{n-2})>0$$

when $k_{n-2}'(0)>0$ and $F_0(\theta_{n-2})>0$.

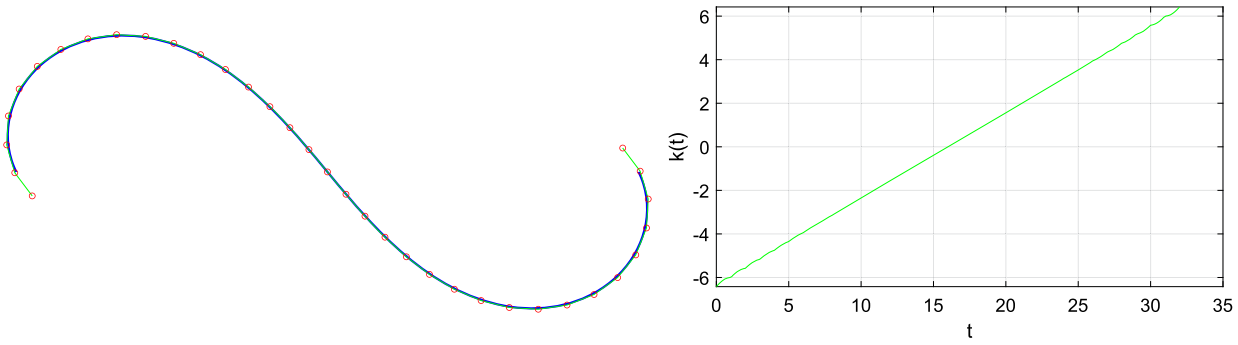

Fig. 4. A cubic Euler B-spline spiral and its curvature plot.

From the expression $F_1'(\theta) = 3\sin(\theta - \frac{\Delta\theta}{2})\sin(\frac{\theta}{2} - \frac{\Delta\theta}{2})$, we know that $F_1'(\theta) > 0$ when $\theta \in [\theta_2, \theta_{i_0}]$. Therefore, we have

$$0 < F_1(\theta_2) < F_1(\theta_3) < \cdots < F_1(\theta_{i_0})$$

when $k_1'(1) > 0$ and $F_1(\theta_2) > 0$. By direct computation, we know that $F_1'(\Delta\theta) = 0$ and $F_1''(\Delta\theta) = \frac{3}{2}\sin\frac{\Delta\theta}{2} > 0$. It follows that $F_1'(\theta) > 0$ when $\theta \in (\Delta\theta, \theta_{n-1}]$. Since $\theta_{i_0+2} = \theta_{i_0+1} + \Delta\theta > \Delta\theta$, we have

$$F_1(\theta_{n-1}) > \cdots > F_1(\theta_{i_0+3}) > F_1(\theta_{i_0+2}) > F_1(\Delta\theta) = 2\sin\frac{\Delta\theta}{2} > 0.$$

This proves the proposition. □

Based on Proposition 3.5, we should just check the signs of $\Delta\theta$, $F_0(\theta_1)$, $F_1(\theta_2)$, $F_0(\theta_{n-2})$ and $F_1(\theta_{n-1})$ to judge the curvature monotonocity of a cubic B-spline curve with Euler control polygon. If these five terms have different signs, the B-spline curve is not a spiral. On the other hand, if the mentioned terms have the same sign, the B-spline curve usually has monotone curvature plot. Fig. 4 illustrates a cubic B-spline curve constructed with 35 control points. When the control points form an Euler polygon and all vertex angles satisfy the conditions stated in Proposition 3.5, the obtained B-spline curve is an Euler B-spline spiral that consists of 32 pieces of cubic spirals.

4. G^1 interpolation by Euler Bézier/B-spline spirals

This section presents algorithms for constructing Euler Bézier spirals or Euler B-spline spirals that interpolate given G^1 Hermite data at the boundaries.

4.1. G^1 interpolation by Euler Bézier spirals

Assume P_a and P_b are two distinctive points on a plane, and T_a and T_b are two unit tangents associated with the points. The goal of G^1 interpolation by an Euler Bézier spiral is to find a Bézier curve $P(t) = \sum_{i=0}^{n} P_i B_{i,n}(t)$, $t \in [0,1]$, such that the Bézier curve satisfies the conditions stated in Proposition 3.1 and interpolates the G^1 Hermite data at the boundaries.

The strategy to construct an Euler Bézier spiral interpolating given G^1 Hermite data consists of following key algorithm steps:

(a) Construct an initial Bézier curve matching the G^1 Hermite data at the boundaries.
(b) Smooth the control polygon of the G^1 interpolating Bézier curve as an Euler polygon.
(c) Elevate the degree of the Bézier curve and re-smooth the control polygon of the curve when the necessary condition for an Euler Bézier spiral is not satisfied.

We explain the details of the algorithm steps. Starting from given boundary data, one can construct an initial Bézier curve of degree n just by choosing $P_0 = P_a$, $P_n = P_b$, $P_1 = P_0 + \lambda T_a$, $P_{n-1} = P_n - \mu T_b$ for some positive numbers λ, μ. Thus the obtained Bézier curve interpolates the given boundary points and matches the given tangent vectors at the ends. Since there may exist multiple spirals interpolating the same set of G^1 Hermite data, the remaining control points of the initial Bézier curve can be chosen to form a polygon with an expected shape. As will be seen in next section, different initial Bézier curves may lead to different final interpolating Bézier spirals.

If the control polygon of a G^1 interpolating Bézier curve is not an Euler polygon, it should be refined or smoothed. The control polygon can be smoothed iteratively, with boundary points and tangents fixed, until an Euler polygon has been obtained or a maximum iteration number has been reached. For each round of smoothing, we first compute the signed vertex angles θ_i, $i = 1, 2, \ldots, n-1$, for the polygon. After then, the angles are refined by linear averaging as

$$\hat{\theta}_i = \frac{1}{3}(\theta_{i-1} + \theta_i + \theta_{i+1}), \quad i = 2, 3, \ldots, n-2. \tag{9}$$

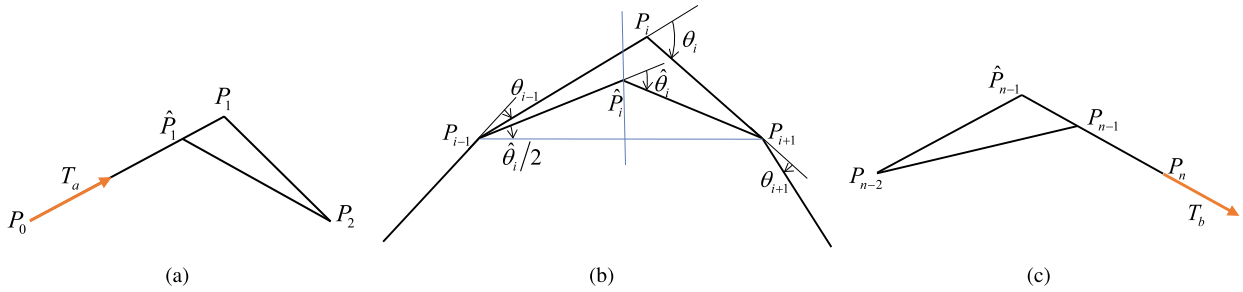

Fig. 5. Smooth the control polygon for a Bézier curve.

Algorithm 1: G^1 interpolation by Euler Bézier spiral.

```
// subroutine for checking an Euler Bézier spiral ;
bool EulerBezierSpiralCheck(P(t)):
    n ← degree of Bézier curve P(t);
    if (the lengths of control polygon edges are not equal) then return FALSE;
    Compute vertex angles θ_i, i = 1,2,...,n−1 ;
    if (max_{1≤i≤n−1}{|θ_i|} > π/2) then return FALSE;
    if (n > 3) then compute θ_DD by Eq. (12); else θ_DD = 0;
    if (θ_DD > 10^{−6}) then return FALSE;
    Compute Δθ, s_0, s_1 by Eq. (13);
    if Δθ, s_0, s_1 have the same sign then
        return TRUE;
    else
        return FALSE;
    end
// subroutine for smoothing the control polygon of a Bézier curve ;
void SmoothingBezierControlPolygon(P(t)):
    n ← degree of Bézier curve P(t);
    if (n <= 3) then return;
    Compute vertex angles θ_i, i = 1,2,...,n−1;
    if (max_{1≤i≤n−1}{|θ_i|} > π/2) then max_count←2; else max_count←10000;
    s_count ← 1; θ_DD ← 10.0; l_ave ← 0; l_bound ← 2‖P_n − P_0‖;
    while (s_count<max_count)&(θ_DD > 10^{−6})&(l_ave < l_bound) do
        for i = 2 to n − 2 do
            Compute filtered vertex angle θ̂_i by Eq. (9);
            Compute refined control point P̂_i by Eq. (10);
        end
        Compute average edge length l_ave;
        Compute refined vertices P̂_1 and P̂_{n−1} by Eq. (11) ;
        Recompute vertex angles θ_i, i = 1,2,...,n−1, and refine θ_DD by Eq. (12);
        s_count++;
    end
// the main procedure ;
void EulerBezierSpiralInterpolation(max_vtx_num):
    input : Boundary points P_a, P_b and boundary tangents T_a, T_b
    output: An Euler Bézier spiral P(t) interpolating the boundary data
    Construct a G^1 interpolating Bézier curve P(t) of degree ≥ 3 ;
    v_num ← number of control points of P(t);
    while (v_num<max_vtx_num)&(EulerBezierSpiralCheck(P(t)) == FALSE) do
        Elevate degree of P(t) by Equation (14);
        SmoothingBezierControlPolygon(P(t));
        v_num++;
    end
    Output (P(t));
```

Linear filtering can guarantee the linearity of the final angles when the smoothing process converges. The vertices P_i, $i = 2, 3, \ldots, n-2$, are then refined to match the filtered angles. Particularly, vertex P_i will be refined to a new position $\hat{P}_i$ such that $\|\hat{P}_i - P_{i-1}\| = \|P_{i+1} - \hat{P}_i\|$ and the angle between vector $\hat{P}_i - P_{i-1}$ and vector $P_{i+1} - \hat{P}_i$ is $\hat{\theta}_i$; see Fig. 5(b). As $\hat{P}_i$ lies on the perpendicular bisector to line segment $P_{i-1}P_{i+1}$ and the angle between line $P_{i-1}\hat{P}_i$ and line $P_{i-1}P_{i+1}$ is $\frac{\hat{\theta}_i}{2}$, the new position of vertex P_i is computed by

$$\hat{P}_i = \frac{P_{i-1} + P_{i+1}}{2} - \tan\frac{\hat{\theta}_i}{2}\mathrm{R}\left(\frac{\pi}{2}\right)\frac{P_{i+1} - P_{i-1}}{2}. \tag{10}$$

To guarantee that the refined Bézier curves still interpolate the given boundary points and have prescribed tangents at the ends, the boundary vertices P_0 and P_n are fixed. Meanwhile, the new position of P_1 or P_{n-1} lies on the tangent line that passes through point P_0 with tangent direction T_a or the tangent line that passes through point P_n with opposite direction of T_b; see Figs. 5(a) and 5(c). As our goal is to construct an Euler polygon with equal length edges, the new positions of P_1 and P_{n-1} are computed by

$$\begin{aligned} \hat{P}_1 &= P_0 + l_{ave} T_a, \\ \hat{P}_{n-1} &= P_n - l_{ave} T_b, \end{aligned} \tag{11}$$

where l_{ave} is the average edge length of current control polygon.

After each round of vertex smoothing, we recompute the vertex angles for the refined control polygon. To check whether or not the control polygon is an Euler polygon, we compute the second order differences of the vertex angles. Let

$$\theta_{DD} = \max_{2 \le i \le n-2} \{|2\theta_i - \theta_{i-1} - \theta_{i+1}|\}. \tag{12}$$

If $\theta_{DD} < 10^{-6}$, the second order differences of the angles are regarded as vanishing and the vertex angles form an arithmetic sequence. Meanwhile, the polygon edges have almost the same length when the vertex angles vary linearly. At this time, the control polygon of the Bézier curve is regarded as an Euler polygon and the smoothing process will be stopped. Otherwise, the control polygon will be smoothed once again. Usually, the smoothing process converges well and stops after a finite number of iterations in practice. In case the iteration number excels a large number, e.g. 10000, the smoothing process will be stopped. Practically, the control polygon of an initial interpolating curve may only consist of a small number of vertices and some vertex angles may be obtuse angles. This kind of interpolating curves can rarely be refined into spirals without adding more control points. To accelerate the smoothing process and improve robustness, the maximum smoothing iteration number can be chosen a small number such as 2 or 5 when $\max_{1 \le i \le n-1}\{|\theta_i|\} > \frac{\pi}{2}$ holds. To keep the updated vertices from deviating too much from initial control polygons, the lengths of polygon edges should be bounded. If the average edge length of current polygon is greater than a predefined bound such as $2\|P_n - P_0\|$, the smoothing process will be stopped.

The curvature monotonicity of a Bézier curve with Euler control polygon can be checked based on Proposition 3.1. Assume the control points of the Bézier curve are still denoted as P_i, $i = 0, 1, \ldots, n$, and the vertex angles of the control polygon are θ_i, $i = 1, 2, \ldots, n-1$. We compute

$$\begin{aligned} \Delta\theta &= (\theta_{n-1} - \theta_1)/(n-2), \\ s_0 &= (n+1)\sin\theta_1 + (n-2)\sin(\theta_1 + \theta_2) - 3(n-1)\sin\theta_1\cos\theta_1, \\ s_1 &= -(n+1)\sin\theta_{n-1} - (n-2)\sin(\theta_{n-2} + \theta_{n-1}) + 3(n-1)\sin\theta_{n-1}\cos\theta_{n-1}. \end{aligned} \tag{13}$$

If the obtained $\Delta\theta$, s_0 and s_1 have different signs, the Bézier curve is not a spiral. We then increase the number of control points of the Bézier curve by degree elevation (Farin, 2001). The new control points are obtained as

$$\bar{P}_i = \frac{i}{n+1} P_{i-1} + \left(1 - \frac{i}{n+1}\right) P_i, \quad i = 0, 1, \ldots, n+1. \tag{14}$$

After then, the control polygon of the reformulated Bézier curve is smoothed again. This process can be iterated, until the computed $\Delta\theta$, s_0 and s_1 have the same sign or a maximum vertex number has been reached. More algorithm details are summarized in Algorithm 1.

4.2. G^1 interpolation by cubic Euler B-spline spirals

The strategy for interpolating G^1 boundary data by cubic Euler B-spline spirals is analogous with that for G^1 interpolation by Euler Bézier spirals. Given boundary points P_a and P_b, together with boundary tangents T_a and T_b, the key steps to construct an interpolating cubic Euler B-spline spiral are as follows:

(a) Construct an initial uniform cubic B-spline curve.
(b) Smooth the control polygon of the B-spline curve such that the polygon becomes an Euler polygon and the obtained B-spline curve interpolates the G^1 boundary data.
(c) Increase the number of control points of the B-spline curve and re-smooth the control polygon when the necessary condition for an Euler B-spline spiral is not satisfied.

Similar to the algorithm for G^1 interpolation by Euler Bézier spirals, the main procedure for G^1 interpolation by cubic Euler B-spline spirals is given in Algorithm 2. The subroutine for checking cubic Euler B-spline spirals and the subroutine for smoothing the control polygon of a B-spline curve are omitted here. These two subroutines can be obtained by minor modifications of subroutine for checking an Euler Bézier spiral or subroutine for smoothing the control polygon of a Bézier curve, which are already given in Algorithm 1.

Given G^1 boundary data, the initial cubic B-spline curve can be constructed freely. It may not necessarily interpolate the given boundary points and boundary tangents. Practically, we can just choose the control polygon of the initial B-spline curve as the control polygon of an interpolating Bézier curve. Though a uniform cubic B-spline curve constructed from the control polygon of an interpolating Bézier curve does not interpolate the prescribed points at the ends, it does define the basic shape of a final interpolating

Algorithm 2: G^1 interpolation by cubic Euler B-spline spiral.

```
// the main procedure ;
void EulerBsplineSpiralInterpolation(max_vtx_num):
    input : Boundary points P_a, P_b and boundary tangents T_a, T_b
    output: A cubic Euler B-spline spiral P(t) interpolating the boundary data
    Construct an initial B-spline curve P(t) with 4 or more control points ;
    v_num ← number of control points of P(t);
    while (v_num<max_vtx_num)&(EulerBsplineSpiralCheck(P(t))==FALSE) do
        Refine and increase the control points for P(t) by Equation (14);
        SmoothingBsplineControlPolygon(P(t));
        v_num++;
    end
    Output (P(t));
```

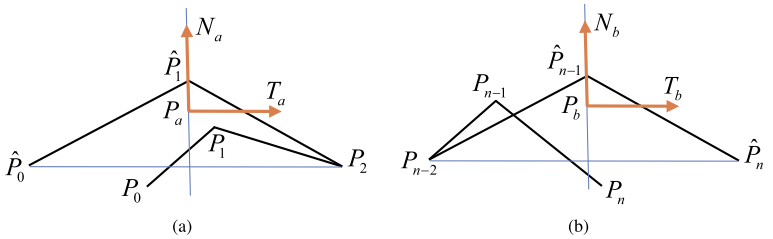

Fig. 6. Refine the boundary control points such that the refined cubic B-spline curve interpolates the G^1 boundary data.

B-spline curve. Since there may exist multiple B-spline spirals interpolating the same set of boundary points and boundary tangents, the control polygon of an initial B-spline curve can be chosen having similar shape just like the expected interpolating spiral.

The goal of the subroutine for smoothing the control polygon of a B-spline curve is to make the control polygon of the curve as an Euler polygon and the obtained cubic B-spline curve interpolates the given points and tangents at the ends. Assume the control points of a current cubic B-spline curve are P_i, $i = 0, 1, \dots, n$. The control points are smoothed using the same technique as that for smoothing the control polygon of an Euler Bézier spiral except the first two and the last two points. By computing the vertex angles θ_i, $i = 1, 2, \dots, n-1$, for the control polygon, the interior control points P_i, $i = 2, 3, \dots, n-2$, are refined by Equation (10) using the filtered angles computed by Equation (9). From the first segment of B-spline curve $C_1(u) = \sum_{j=0}^{3} P_j N_{j,4}(u)$, $u \in [0, 1]$, we know that $C_1'(0) = \frac{1}{2}(P_2 - P_0)$ and $C_1(0) = \frac{1}{6}P_0 + \frac{2}{3}P_1 + \frac{1}{6}P_2$. To guarantee that the tangent direction of the refined B-spline curve at the starting point is parallel to vector T_a, the refined boundary control point $\hat{P}_0$ should satisfy $P_2 - \hat{P}_0 \| T_a$. Let $l_a = (P_2 - P_a) \cdot T_a$. The boundary point P_0 is refined by

$$\hat{P}_0 = \begin{cases} P_2 - 2l_a T_a, & \text{if } l_a > 0 \\ P_a + l_a T_a, & \text{otherwise} \end{cases}$$

This choice of $\hat{P}_0$ can guarantee $\|P_a - \hat{P}_0\| = \|P_a - P_2\|$ when $l_a > 0$ and keep the end tangent of the obtained B-spline curve from having opposite direction with T_a when $l_a < 0$. Let $N_a = \mathrm{R}(\frac{\pi}{2})T_a$. Based on the assumption that $\|\hat{P}_1 - \hat{P}_0\| = \|P_2 - \hat{P}_1\|$, we assume that $\hat{P}_1 = P_a + h_a N_a$; see Fig. 6(a). When the cubic B-spline curve interpolates P_a at the end, it yields

$$P_a = \frac{1}{6}\hat{P}_0 + \frac{2}{3}\hat{P}_1 + \frac{1}{6}P_2.$$

From this equation we have

$$P_a - \frac{1}{2}(\hat{P}_0 + P_2) = 2h_a N_a.$$

Dot either side of the equation by N_a, we have $h_a = \frac{1}{2}[P_a - \frac{1}{2}(\hat{P}_0 + P_2)] \cdot N_a$.

In the same way as the refinement of first two control points, the last two control points are also refined based on the G^1 interpolation at the end; see Fig. 6(b). Let $l_b = (P_{n-2} - P_b) \cdot T_b$. Point P_n is first refined as

$$\hat{P}_n = \begin{cases} P_{n-2} - 2l_b T_b, & \text{if } l_b < 0 \\ P_b + l_b T_b, & \text{otherwise} \end{cases}$$

Let $N_b = \mathrm{R}(\frac{\pi}{2})T_b$. Point P_{n-1} is then refined as

$$\hat{P}_{n-1} = P_b + h_b N_b,$$

where $h_b = \frac{1}{2}[P_b - \frac{1}{2}(P_{n-2} + \hat{P}_n)] \cdot N_b$.

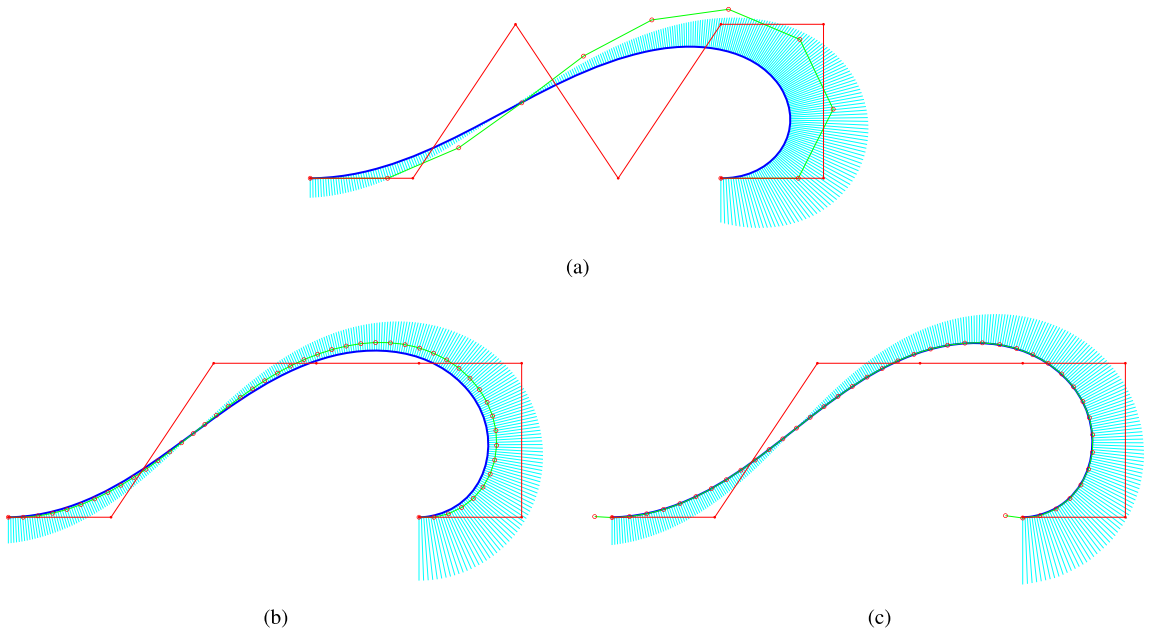

Fig. 7. Interpolation of a pair of G^1 Hermite data that lie on a line and have opposite tangent directions by various curves: (a) a degree 10 Bézier curve with Euler control polygon; (b) an Euler Bézier spiral of degree 48; (c) a cubic Euler B-spline spiral with 43 control points. In this and following examples the circles '∘' denote the control points of the interpolating Bézier or B-spline curves while the solid dots '•' denote the vertices of initial control polygons that match the given boundary data. The cyan lines indicate the curvature combs of the interpolating curves. (For interpretation of the colors in the figure(s), the reader is referred to the web version of this article.)

If $l_a > 0$ and $l_b < 0$, the refined B-spline curve interpolates P_a, P_b and has tangents T_a, T_b at the two end points; otherwise, the B-spline curve may not interpolate the given boundary data. If the control polygon of an interpolating B-spline curve is not an Euler polygon or the obtained curve does not interpolate the prescribed end points and end tangents, the polygon will be smoothed again. This process stops until an interpolating B-spline curve with Euler control polygon is obtained or a maximum iteration number has been reached. Similar to G^1 interpolation by Euler Bézier spirals, the iteration will be stopped when the average edge length of current polygon is greater than a predefined bound, e.g. $2\|P_b - P_a\|$. Practically, the smoothing process converges well and a G^1 interpolating cubic B-spline curve with Euler control polygon can be obtained after dozens or hundreds times of polygon smoothing.

The check of curvature monotonicity of a G^1 interpolating cubic B-spline curve with Euler control polygon is similar with that for a Bézier curve. Instead of Proposition 3.1, we verify the signs of curvature derivatives based on Proposition 3.5. Particularly, we should check the signs of $\Delta\theta$, $F_0(\theta_1)$, $F_1(\theta_2)$, $F_0(\theta_{n-2})$ and $F_1(\theta_{n-1})$ as defined in Proposition 3.5. If these five terms have the same sign, the interpolating B-spline curve is regarded as an Euler B-spline spiral; otherwise, the B-spline curve is not a spiral. If a B-spline curve is checked as a non-spiral curve, the control points are refined by Equation (14). In our experiments, even if the vertex angles satisfy conditions stated in Proposition 3.5 but $|\theta_1| > 0.1\pi$ or $|\theta_{n-1}| > 0.1\pi$, we still refine and add more control points for the B-spline curve. When the control points have been increased, the control polygon will be re-smoothed by the subroutine for polygon smoothing. This process continues until an Euler B-spline spiral with bounded vertex angles is obtained or a maximum iteration number has been reached. Euler B-spline spirals with bounded vertex angles are usually much fairer than B-spline spirals just with monotone curvature profiles.

Fig. 7 illustrates examples of G^1 interpolation by the proposed algorithms. Given two points together with two opposite unit tangents on a line, a polygon consisting of 8 vertices is first constructed to interpolate the G^1 boundary data; see Fig. 7(a). Though the initial control polygon has several obtuse vertex angles with different signs, a degree 10 Bézier curve with Euler control polygon is obtained after 3 rounds of degree elevation and polygon smoothing by employing Algorithm 1. It is checked that the vertex angle difference $\Delta\theta$ of the control polygon of the interpolating Bézier curve has the same sign with the curvature derivative $k'(0)$ but an opposite sign with $k'(1)$. Since the necessary condition stated in Proposition 3.1 is not satisfied, the obtained Bézier curve is not a spiral. As the control polygon is an Euler polygon, the Bézier curve still has a pleasing looking shape. In Fig. 7(b) we first interpolate the G^1 Hermite data by a modified initial polygon. By employing Algorithm 1 and choosing a large bound for the vertex number, the procedure stops and an interpolating Euler Bézier spiral of degree 48 is obtained when the computed $\Delta\theta$, $k'(0)$ and $k'(1)$ have the same sign. Starting from the same initial control polygon as in Fig. 7(b), a G^1 interpolating cubic Euler B-spline spiral with 43 control points is obtained by employing Algorithm 2; see Fig. 7(c) for the interpolating curve. By computing curvatures at densely sampled points on the interpolating Bézier or B-spline curves, we see that the obtained Euler Bézier spiral and Euler B-spline spiral do have monotone curvature plots even though they are constructed based on some necessary conditions.

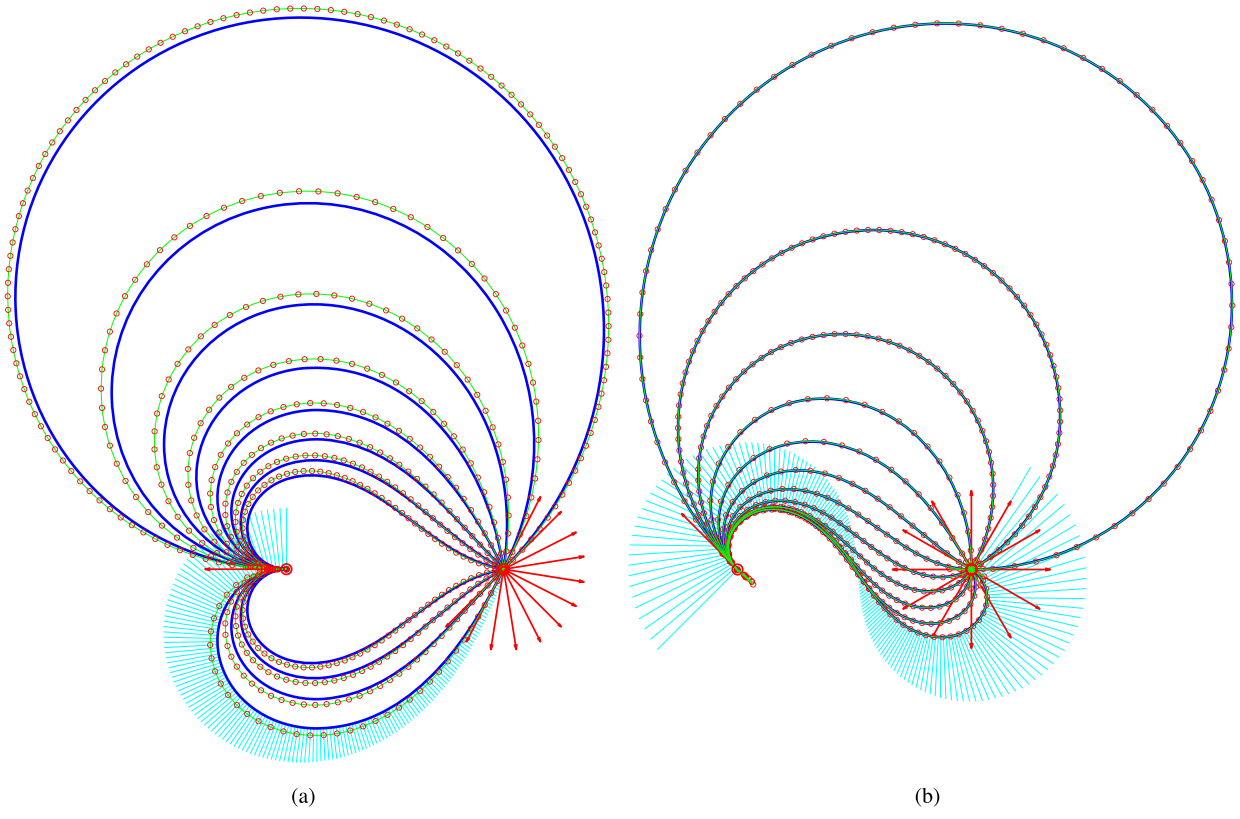

Fig. 8. Interpolation of G^1 Hermite data by (a) Euler Bézier spirals, or (b) cubic Euler B-spline spirals. For clarity purpose, only the curvature combs for the last interpolating Euler Bézier spiral or the last interpolating Euler B-spline spiral have been plotted.

5. Experimental examples

In this section we present several interesting examples to show the results of geometric Hermite interpolation by Euler Bézier spirals or Euler B-spline spirals.

Firstly, we interpolate prescribed geometric Hermite data by Euler Bézier spirals or Euler B-spline spirals with default choices of initial control polygons. For two given boundary points $P_a = (-1,0)^T$ and $P_b = (1,0)^T$, the boundary tangents are chosen as $T_a = (-1,0)^T$ and $T_b = (\cos(-0.75\pi + \frac{k\pi}{10}), \sin(-0.75\pi + \frac{k\pi}{10}))^T$, $k = 0,1,\ldots,11$. For each pair of geometric Hermite data $(P_a,T_a),(P_b,T_b)$, the control points of an initial cubic interpolating Bézier curve are given by $P_0 = P_a$, $P_1 = P_0 + 0.35 l_e T_a$, $P_2 = P_b - 0.35 l_e T_b$, $P_3 = P_b$, where $l_e = \|P_b - P_a\|$. By employing Algorithm 1, Euler Bézier spirals of degree 122, 58, 46, 41, 40, 41, 43, 46, 46, 43, 41, 40 are obtained to interpolate the given Hermite data, respectively. See Fig. 8(a) for the boundary data and the interpolating Euler Bézier spirals. Keeping P_a and P_b unchanged, we then choose $T_a = (\cos(0.75\pi), \sin(0.75\pi))^T$ and $T_b = (\cos(-\pi + \frac{k\pi}{6}), \sin(-\pi + \frac{k\pi}{6}))^T$, $k = 0,1,\ldots,11$. By the same technique as Euler Bézier spirals, initial control polygons each consists of four vertices are computed based on the geometric Hermite data. Employing Algorithm 2, cubic Euler B-spline spirals consisting of 77, 87, 62, 29, 25, 27, 31, 35, 38, 42, 44, 53 control points are obtained to interpolate the geometric Hermite data, respectively. See Fig. 8(b) for the interpolating curves.

Secondly, we interpolate G^1 boundary data by Euler Bézier spirals. Assume the boundary points are $P_a = (0,0)^T$ and $P_b = (1.25,0)^T$ and the unit tangents at the two points are $T_a = (-1,0)^T$ and $T_b = (0,-1)^T$, respectively. To interpolate the given boundary data by an Euler Bézier spiral, a convex control polygon that consists of 7 control points is first constructed to match the boundary data. Starting from the initial control polygon, a convex Euler Bézier spiral of degree 43 is obtained by employing Algorithm 1; see Fig. 9(a) for the interpolating Bézier spiral. By keeping the end points and end tangents unchanged, the initial control polygon has been modified as an inflectional polygon; see Fig. 9(b). As a result, an Euler Bézier spiral of degree 66 is obtained to interpolate the prescribed boundary data. Differently from the convex Euler Bézier spiral illustrated in Fig. 9(a), the interpolating Euler Bézier spiral in Fig. 9(b) has an inflection point.

Thirdly, we interpolate G^1 boundary data by cubic Euler B-spline spirals. We choose the boundary points $P_a = (-1,0)^T$ and $P_b = (1,-0.5)^T$, and choose the tangents at the two boundary points as $T_a = T_b = (-\sqrt{2}/2, -\sqrt{2}/2)^T$. Same as G^1 interpolation by Euler Bézier spirals, rough initial control polygons are first constructed to interpolate the given boundary data. Since the two boundary tangents are the same, it is expected that the interpolating spirals are inflectional. Starting from the G^1 boundary data, two initial control polygons with 4 or 9 control points are constructed to match the boundary data. By employing Algorithm 2, two

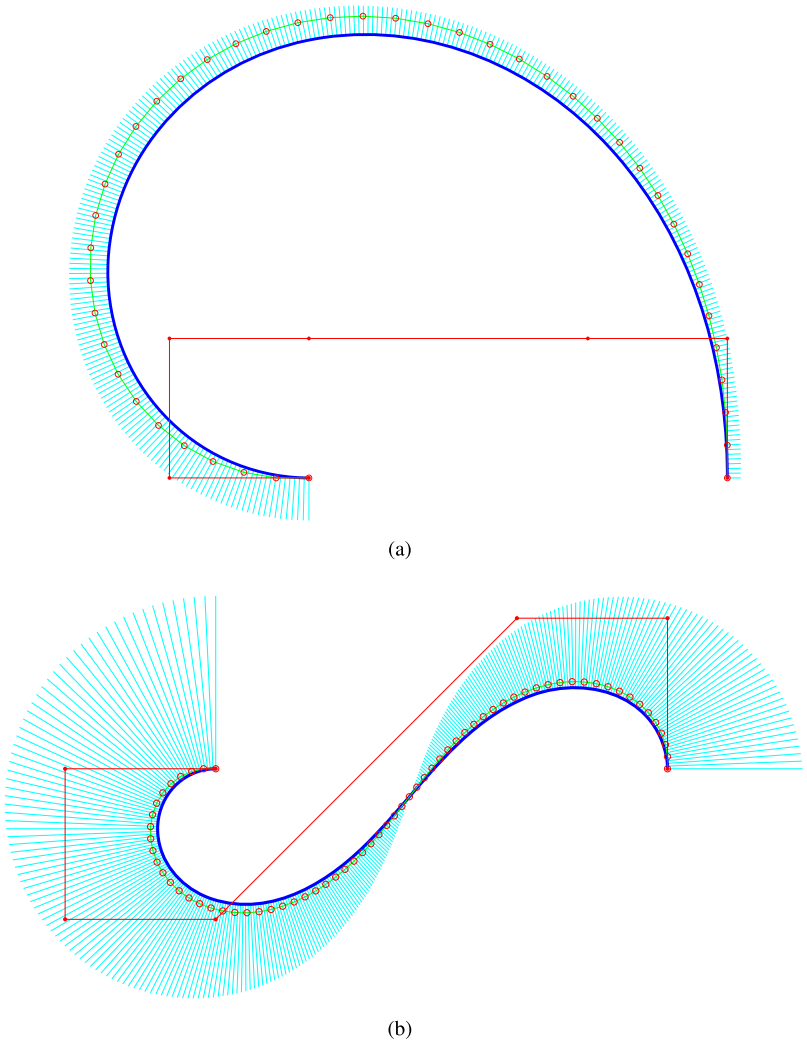

Fig. 9. Interpolation of G^1 boundary data by Euler Bézier spirals: (a) the interpolating Euler Bézier spiral of degree 43; (b) the interpolating Euler Bézier spiral of degree 66.

cubic Euler B-spline spirals with 42 or 105 control points are obtained to interpolate the prescribed boundary data; see Fig. 10 for the initial control polygons and final interpolating B-spline curves.

Lastly, we construct a rotational surface by rotating an interpolating cubic Euler B-spline spiral. Assume the G^1 boundary are defined by a polygon consisting of vertices $(-0.4,-1.5)^T$, $(-0.8,-1.5)^T$, $(-0.3,0.6)^T$ and $(-0.6,1.5)^T$ on the xz-plane. By using the same technique as the last example, a cubic Euler B-spline spiral consisting of 24 control points is obtained to interpolate the boundary points and boundary tangents that are defined by the initial rough polygon. See Fig. 11(a) for the interpolating B-spline curve. By rotating the Euler B-spline spiral along the z-axis, we obtain a rotational surface as illustrated in Fig. 11(b). The isophote lines in Fig. 11(b) and Gaussian curvature plot in Fig. 11(c) show the smoothness and fairness of the rotational surface.

6. Conclusions and future work

In this paper we have proposed to define Euler Bézier spirals and Euler B-spline spirals by using Euler polygons that have equal length edges and linear varying vertex angles. Euler Bézier spirals and Euler B-spline spirals can have approximately linear varying curvature plots when the vertex angles of control polygons satisfy some simple necessary conditions. Interpolation of prescribed G^1 boundary data by the proposed curve models can be implemented in a simple but efficient way. Due to their quality and simplicity, Euler Bézier spirals and Euler B-spline spirals can be applied in NURBS based CAD systems as well as somewhere conventional Euler spirals have been applied.

At present, the curvature monotonicity of all computed Euler Bézier spirals and Euler B-spline spirals have been successfully verified by dense sampling of curvature functions. Even so, a rigorous proof of the curvature monotonicity under the proposed necessary conditions for the construction of Euler Bézier spirals or Euler B-spline spirals is still an open problem which should be

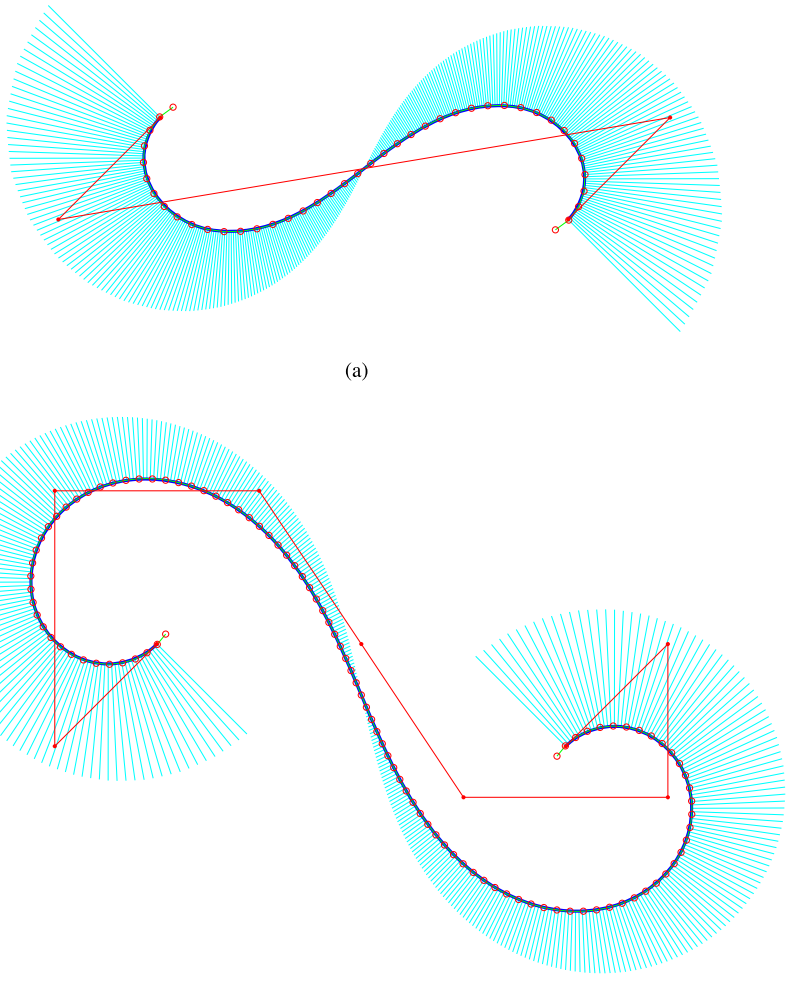

Fig. 10. Interpolation of G^1 boundary data by Euler B-spline spirals: (a) the interpolating cubic Euler B-spline spiral with 42 control points; (b) the interpolating cubic Euler B-spline spiral with 105 control points. The boundary points and boundary tangents are given by the boundary legs of the initial red polygons.

studied further in the future. As another future work, definitions and applications of Euler rational Bézier spirals and Euler rational B-spline spirals in 2D or 3D space also deserve further study.

CRediT authorship contribution statement

Xunnian Yang: Conceptualization, Software, Writing – original draft, Writing – review & editing.

Declaration of competing interest

The authors declare that they have no known competing financial interests or personal relationships that could have appeared to influence the work reported in this paper.

Data availability

Data will be made available on request.

Acknowledgement

We owe thanks to anonymous reviewers for valuable comments and suggestions. This work was supported by the National Natural Science Foundation of China under Grant No. 12171429.

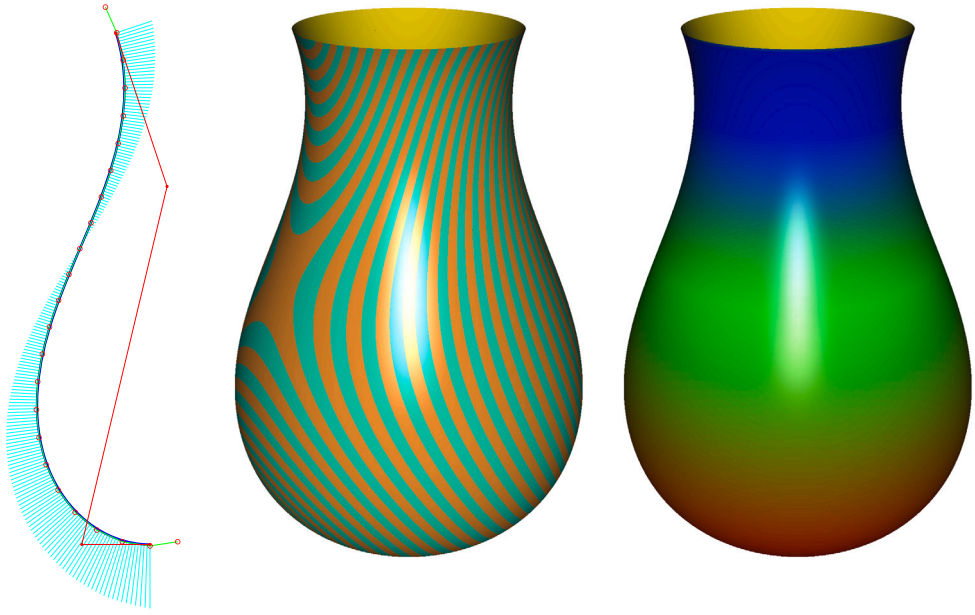

Fig. 11. (a) The G^1 interpolating cubic Euler B-spline spiral on the xz-plane; (b) the surface obtained by rotating the Euler B-spline spiral along the z-axis and the isophote lines of the surface; (c) Gaussian curvature plot of the rotating surface, where red, green or blue colors represent positive, zero or negative curvatures of the surface.

References

Baran, I., Lehtinen, J., Popovic, J., 2010. Sketching Clothoid splines using shortest paths. Comput. Graph. Forum 29 (2), 655–664.

Bertolazzi, E., Frego, M., 2015. G^1 fitting with clothoids. Math. Methods Appl. Sci. 38, 881–897.

Cantón, A., Fernández-Jambrina, L., Vázquez-Gallo, M.J., 2021. Curvature of planar aesthetic curves. J. Comput. Appl. Math. 381, 113042.

Chen, Y., Cai, Y., Zheng, J., Thalmann, D., 2017. Accurate and efficient approximation of Clothoids using Bézier curves for path planning. IEEE Trans. Robot. 33 (5), 1242–1247.

Dietz, D.A., Piper, B.R., 2004. Interpolation with cubic spirals. Comput. Aided Geom. Des. 21 (2), 165–180.

Farin, G., 2001. Curves and Surfaces for CAGD: A Practical Guide, fifth edition. Morgan Kaufmann.

Farin, G.E., 2006. Class A Bézier curves. Comput. Aided Geom. Des. 23 (7), 573–581.

Farouki, R.T., Pelosi, F., Sampoli, M.L., 2021. Approximation of monotone clothoid segments by degree 7 Pythagorean-hodograph curves. J. Comput. Appl. Math. 382, 113110.

Frey, W.H., Field, D.A., 2000. Designing Bézier conic segments with monotone curvature. Comput. Aided Geom. Des. 17 (6), 457–483.

Havemann, S., Edelsbrunner, J., Wagner, P., Fellner, D.W., 2013. Curvature-controlled curve editing using piecewise clothoid curves. Comput. Graph. 37 (6), 764–773.

Kimia, B.B., Frankel, I., Popescu, A., 2003. Euler spiral for shape completion. Int. J. Comput. Vis. 54 (1–3), 159–182.

Mineur, Y., Lichah, T., Castelain, J.M., Giaume, H., 1998. A shape controlled fitting method for Bézier curves. Comput. Aided Geom. Des. 15 (9), 879–891.

Montés, N., Herraez, A., Armesto, L., Tornero, J., 2008. Real-time clothoid approximation by rational Bézier curves. In: 2008 IEEE International Conference on Robotics and Automation, ICRA 2008, May 19-23, 2008, Pasadena, California, USA. IEEE, pp. 2246–2251.

Romani, L., Viscardi, A., 2021. Planar Class A Bézier curves: the case of real eigenvalues. Comput. Aided Geom. Des. 89, 102021.

Saito, T., Yoshida, N., 2023. Curvature monotonicity evaluation functions on rational Bézier curves. Comput. Graph. 114, 219–228.

Sánchez-Reyes, J., Chacón, J.M., 2003. Polynomial approximation to clothoids via s-power series. Comput. Aided Des. 35 (14), 1305–1313.

Tong, W., Chen, M., 2021. A sufficient condition for 3D typical curves. Comput. Aided Geom. Des. 87, 101991.

Walton, D.J., Meek, D.S., 2009. G^1 interpolation with a single cornu spiral segment. J. Comput. Appl. Math. 223, 86–96.

Wang, A., He, C., Zheng, J., Zhao, G., 2023. 3D Class A Bézier curves with monotone curvature. Comput. Aided Des. 159, 103501.

Wang, L., Miura, K.T., Nakamae, E., Yamamoto, T., Wang, T.J., 2001. An approximation approach of the clothoid curve defined in the interval $[0, \pi/2]$ and its offset by free-form curves. Comput. Aided Des. 33 (14), 1049–1058.

Wang, Y., Zhao, B., Zhang, L., Xu, J., Wang, K., Wang, S., 2004. Designing fair curves using monotone curvature pieces. Comput. Aided Geom. Des. 21, 515–527.

Ynchausti, C., Brown, N., Magleby, S.P., Bowden, A.E., Howell, L.L., 2022. Deployable Euler spiral connectors. J. Mech. Robot. 14 (2), 021003.

Yoshida, N., Hiraiwa, T., Saito, T., 2008. Interactive control of planar Class A Bézier curves using logarithmic curvature graphs. Comput-Aided Des. Appl. 5 (1–4), 121–130.

Zhou, H., Zheng, J., Yang, X., 2012. Euler arc splines for curve completion. Comput. Graph. 36 (6), 642–650.